

The Dust Temperature of the “Dusty” Radio Galaxy MG 1019+0535: Evidence for an Outflow

Curtis Manning & Hyron Spinrad
 Department of Astronomy, University of California at Berkeley
 Berkeley, CA 94720
 email: (cmanning,spinrad)@bigz.berkeley.edu

ABSTRACT

Radio galaxies characteristically have strong Ly α emission lines. However, a few have Ly α equivalent widths that are substantially weaker in relation to other emission lines. One in particular was studied by Dey et al. (1995), MG 1019+0535 ($z = 2.765$). We report on our reduction of Infrared Space Observatory (*ISO*) data in the 160 μm -band for this galaxy. We also compile information on two other high redshift active galaxies with weak Ly α lines, the radio galaxy TXS 0211–122, and the AGN–starburst galaxy F 10214+4724, to provide a small weak-Ly α line sample. IRAS plus *ISO* data show that F 10214+4724 has a temperature 89 ± 12 K. TXS 0211–122 was not detected in either the submillimeter or microwave. Submillimeter measurements of MG 1019+0535 (Cimatti et al., 1998) were suggestive of a dust temperature in the range $35 \text{ K} \leq T_d \leq 80 \text{ K}$. However our $2\text{-}\sigma$ upper limit on the flux at 160 μm shows that $T_d \lesssim 32 \text{ K}$. An energy argument based on observations which constrain the total optical extinction strongly suggests that the dust temperature must be even lower; $T_d \lesssim 20 \text{ K}$. We find the contrast between the high-temperature dust in the active starburst galaxy and the low-temperature dust in the evolved, albeit active galaxy, is consistent with an expanding cloud of dust. We find that the temperature range can be reconciled if we are seeing MG 1019+0535 at a post-starburst age of $\approx 500 - 700 \text{ Myr}$, with the bulk of its dust cloud at a galactocentric distance $R_d \gtrsim 300 \text{ kpc}$.

Subject headings: Cosmology: observations — galaxies:active — galaxies: evolution — galaxies: starburst — dust, extinction

1. Introduction

Though the role of dusty H I clouds in the quenching of the Ly α line of star forming galaxies is by now well-recognized (Neufeld, 1991; Chen & Neufeld, 1994; Legrand et al., 1997; Kunth et al., 1998), how it is manifested in specific galaxies is not well-understood. Real progress on the observational side of the problem began with the launch of the *Infrared Astronomy Satellite* (IRAS). With its detectors tuned to 12, 25, 60 and 100 μm , it was sensitive to dust emission at moderate temperatures from galaxies in the low-redshift universe. The dust emission at these wavelengths may be used to determine the spatial extent of dust and help constrain the total extinction occurring in the galaxy. The often tantalizing data emerging from IRAS led to the planning and implementation of more sensitive detectors, both ground- and space-based. The Infrared Space Observatory (*ISO*)¹, was designed to give higher spatial and spectral resolution and greater

¹ISO is an ESA project with instruments funded by ESA Member States (especially the PI countries: France, Germany, the Netherlands and the United Kingdom) with the participation of ISAS and NASA.

sensitivity over this far-infrared (FIR) range. Astronomy now appears to be approaching a “golden age” of FIR observation, as telescopes, observatories, and instruments, such as SCUBA, MIPS on SIRTf, and SPIRE on FIRST, are implemented.

How is dust produced, and what is its fate? A very simplified model of dust production in galaxies starts with gasses expelled from evolved stars — supernovae and winds from evolved, metal-enriched stars. This enriched gas forms dust when condensing molecules collide and adhere. The probability for survival of a small grain is largely dependent on the number density and energy of ambient UV photons; the absorption of a single UV photon can vaporize a small grain. A burst of star formation may cause large-scale winds which carry dust to large galactocentric distances (Legrand et al., 1997; Frye & Broadhurst, 1998; Warren et al., 1998; Kunth et al., 1998). In addition, the expelled dust may be propelled by photon pressure and corpuscular drag (Burns et al., 1979). The increased incidence of FIR/sub-mm emission from dust in radio galaxies with increased redshift (Archibald et al., 2000) suggests that these galaxies were rich in warm dust shortly after the star-forming episode which formed them, but also that in time, the dust is dispersed. This implies that the efficiency of the galactic dust in absorbing optical radiation declines strongly with time following a starburst, leading to a declining color excess.

One study of IRAS fluxes in galaxy disks (Lonsdale Persson & Helou, 1987) found two distinct dust components; a warm component associated with OB associations and HII regions, and a cool component associated with a neutral ISM. Similarly, recent studies (Calzetti, 1999; Calzetti et al., 2000) find that dust in nearby star-forming galaxies can often be fit by two-components – a warm (typically $T \approx 40 - 55$ K), and a cool ($T \approx 20 - 23$ K) component. A wavelength dependence of the dust emissivity ($\alpha \sim \nu^\epsilon$) produces a modified Planck function with a luminosity proportional to $T_d^{4+\epsilon}$, where ϵ is the dust emissivity index, usually taken to be in the range $1 \leq \epsilon \leq 2$. Galactic dust has an emissivity index that increases slowly from the Rayleigh-Jeans tail, toward a value $\sim \nu^2$ near the maximum, and is well-fit by an emissivity $\sim \nu^{1.7}$ with a median dust temperature $T_d \simeq 19$ K (Finkbeiner et al., 1999). However, the fits to local star-forming galaxies by Calzetti et al. (2000) is well-approximated by an $\epsilon \sim 2$. Calculations of dust mass in low redshift, actively star-forming galaxies (Calzetti et al., 2000), find that the cool dust mass may often be more than two orders of magnitude larger than the warm component. Yet because of the strong wavelength dependence of the emission, the warm component is usually more luminous. A high dust opacity has been cited as a factor in the production of cool clouds (Calzetti et al., 2000), though in the absence of a warm component it may be reasonable to conjecture that the low dust temperature is due to its having been blown to large galactocentric distances in a post-starburst galaxy.

We now apply these concepts to radio galaxies. Radio galaxies are often viewed as a sub-population of elliptical galaxies (Matthews et al., 1964; McLure et al., 1999). As a group, ellipticals show few signs of significant amounts of dust in the lower-redshift universe. But at high-redshift, closer to the epoch of galaxy formation, it may be possible to see the signs of large amounts of dust in radio galaxies. One method of detecting this dust is to observe the strength of its Ly α emission line relative to other emission lines. In their study of the radio galaxy MG 1019+0535 ($z=2.765$), Dey et al. (1995) discussed the implications of the observed low flux in the Ly α line in relation to that of He II λ 1640 and pondered the role of dust in the apparent selective extinction of its Ly α line. They found that relative to the He II λ 1640 line, the observed Ly α line strength is only $\sim 10\%$ relative to that of the composite 3CR radio galaxy spectrum of McCarthy (1993). Dey et al. (1995) also discussed the radio galaxy TXS 0211–122 ($z = 2.340$), and IRAS galaxy (and faint radio source) F 10214+4714 ($z = 2.286$), both of which have weak Ly α to He II λ 1640 ratios $< 2.5\%$, and 15% , respectively.

Because the Ly α line center of MG 1019+0535 is redshifted relative to other permitted lines, Dey et al.

(1995) proposed a scenario in which the dust cloud lies outside the line-emitting region, perhaps propelled away by winds. Dust has a well-modeled, broad effect on optical spectra, producing a spectral reddening by its wavelength-dependent extinction of photons. However, if neutral hydrogen is associated with the dust cloud, then Ly α photons will experience a much greater extinction due to their increased path-length in the cloud arising from their resonance with H I.

In an attempt to detect emission from the postulated dust cloud, we observed MG 1019+0535 with the Infrared Space Observatory (ISO). Using this, and sub-millimeter data from the literature, we investigate its dust content and temperature in relation to measures of its optical extinction. We also retrieved archival ISO data on TXS 0211–122 and F 10214+4724 which we use to compare with our results on MG 1019+4724.

The paper is organized as follows: In §2 we present the ISO data for the three galaxies. In §3 we describe the reduction of ISO data, and introduce other, submillimeter and IRAS data in order to derive dust temperatures. In §4 we attempt an energetic reconciliation of the FIR, with the optical data. In §5 and §6 we discuss our findings, and present our conclusions.

Throughout this paper we assume an Einstein-De Sitter cosmology with $H_0 = 50 \text{ km s}^{-1} \text{ Mpc}^{-1}$, unless otherwise noted.

2. ISO Data

2.1. MG 1019+0535

Our observations of MG 1019+5035 were made with ISOPHOT, the imaging photopolarimeter on-board ISO, in observing mode PHT 22. ISOPHOT offers multi-filter photometry in two mosaic arrays, equipped with filters in wavelength bands ranging from 50 to 100 microns (the C100 detector, a 3 by 3 pixel grid), and 120 to 200 microns (the 2 by 2 pixel C200 detector). Preceding and following each measurement of the galaxy, observations of an internal Fine Calibration Source (FCS) are made. The FCS measurements are designed to act as a stable reference source to be used for calibration of the data. Experiments are generally designed so that the standard source is heated to a temperature which will give a flux at the detectors approximately equal to that expected from the astrophysical source plus background. This is because there is a large temporal lag in the sensitivity stabilization for large changes in flux. Observations were made through the 50, 90, and 160 μm -band filters. For reasons explained below, we only use the 160 μm data, a filter which is centered at 174 μm . Two measurements were made, a 256 s exposure, then a second exposure, spatially offset from each other by 90'' in declination, for 128 s.

As we shall see, analysis of the images shows that the calibration of the data is not satisfactory, perhaps due to a non-linearity in the response of the detectors to different flux levels. One result, clearly seen in the 160 μm data, is a wide variance among the individual pixels of these observations whose pixel-specific values do not significantly change when the telescope pointing is changed. Unfortunately these systematic variations are not constant in time, and so cannot be modeled by recourse to other data except by considering observations which are in close temporal proximity. However, only the 160 μm data had different pointings, so that the 60 and 90 μm data cannot be corrected for these problems.

2.2. TXS 0211–122 and F 10214+4724

ISO data for TXS 0211–122 and F 10214+4724 were available from the archives (<http://ines.vilspa.esa.es/> or <http://www.ipac.caltech.edu/iso/>). These data were taken in P32 mode, which produces a chopped map. We discuss this more thoroughly in §§3.4 and 3.5.

3. Data Reduction

3.1. MG 1019+4724

We will describe the reduction of the ISO data for MG 1019+0535 in detail, as it is unconventional. As noted above, we consider only the 160 μm C200 data. ISOPHOT data is reduced using standard PHT Interactive Analysis (PIA) software, a software package developed specifically for the reduction of ISOPHOT data. To distinguish calibrator measurements from those of the astrophysical object, we refer to the former as *FCS*, and the latter as *source* measurements.

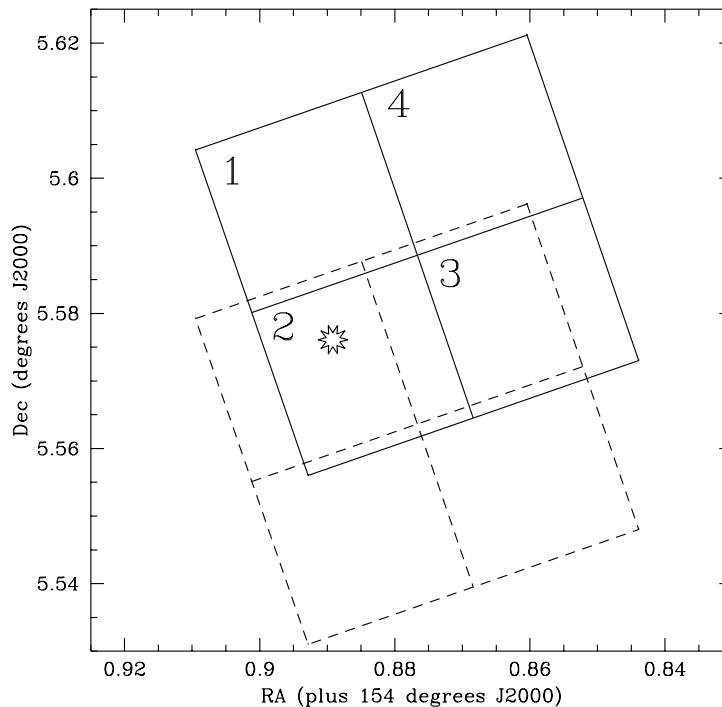


Fig. 1.— The placement of the C200 detectors in the sky relative to MG 1019+0535, symbolized by the star. The radio galaxy is reasonably close to the center of the pixel in which it resides. Numbers show pixel numbers, referred to in the text. Each pixel is about $90''$ square; the airy disk in the 160 μm -band filter has a radius of $\sim 67''$.

Figure 1 shows the placement of the detectors on the sky during the two source measurements. As can be seen, MG 1019+0535 was in pixel #2 during the first measurement, and pixel #1 in the second. We expect that any significant flux density in the 160 μm -band from the radio galaxy would be betrayed

by a different pattern in the two measurements. We reduced the data to the point just before the flux calibration, then studied both the FCS and source data. We noticed that specific pixel values were very consistent between successive observations, but among themselves, pixel values varied by as much as $\sim 40\%$. The two source observations of MG 1019+0535 also show a wide variation in values among pixels of a given measurement, and which are also highly consistent between measurements. However, the pixel ranking is different between FCS, and source measurements. The mean pixel values of the source measurements of observations #1 and #2 are different by $\sim 4\%$. This is in all probability attributable to an internal systematic effect due to the different length of the observations (256, and 128 s, respectively). By normalizing the means of the source, and FCS measurements between observations #1 and #2, it is found that the average variation within the individual pixels in the two measurements is reduced to on order 1.2%, and 1.4% of the mean normalized source, and FCS measurements, respectively.

Three preliminary conclusions can be drawn from this data. First, there is a clear consistency between the sets of FCS and source measurements. Second, taken together with the large variance of values between pixels of both source and FCS measurements, this suggests either a severe non-linearity in the response to an energy source, variations in detector response between pixels, or additional sources of systematic error. Finally, the very small variation of measurements of the source as a function of pixel number, taken together with the movement of the telescope (see Fig. 1) implies that the source radio galaxy does not make a significant contribution to the flux detected in the pixels. Therefore, a good first approximation would appear to be that there is no sign of a signal from the source galaxy. Subsequent manipulation of the data appears to confirm this conclusion.

3.2. Procedures for Further Calibration of MG 1019+0535 Data

In order to test for the existence of a signal of the radio galaxy in the data, we formed the null hypothesis that there was no signal. Since geometric factors are involved in the calibration process, it was thought wise to use the calibrated data (which uses the sensitivity function derived from the FCS measurements) as a basis for further reductions. The fact that the radio galaxy is in pixel 2 in the first, and in pixel 1 in the second measurement, should enable our hypothesis to be invalidated.

Table 1 shows the sequence of calibration. Step 1 shows the fluxes in MJy sr⁻¹ following calibration of the data. In step 2, we normalize the flux densities of observation #2 to those of observation #1 by multiplying the pixel values in the former by the ratio of the mean of the pixels in the first source measurement to that in the second, a reduction of $\sim 4\%$. We normalize measurement #2 to #1, rather than the reverse because #1 has a twice longer exposure, and is thus more likely to be correct. The third step corrects for the apparent variation in sensitivity of each pixel; each pixel count in step 2 is multiplied by the average of all pixels in step 2 divided by the pixel-specific average between measurements. Finally, in step 4 we subtract off the mean. Note that step 3 has the effect of making the deviations from zero symmetric between measurements 1 and 2. We discuss this more extensively below. In Table 1, the data are presented in units of MJy/sr. The asterisks denote the presence of the radio galaxy in that pixel.

Pixel No.	Step One		Step Two		Step Three		Step Four	
	Meas. 1	Meas. 2	Meas. 1	Meas. 2	Meas. 1	Meas. 2	Meas. 1	Meas. 2
1	7.66	7.93*	7.66	7.627*	5.888	5.862*	0.013	-0.013*
2	5.38*	5.55	5.38*	5.341	5.891*	5.895	0.016*	-0.016
3	6.12	6.49	6.12	6.234	5.826	5.925	-0.049	0.049
4	4.34	4.47	4.34	4.298	5.903	5.847	0.028	-0.028

Table 1 : The reduction of data in units of MJy sr^{-1} . See the text for a discussion of the steps. The asterisk denotes the pixel in which MG 1019+0535 was located during the measurement.

Referring to the final step of Table 1, one can see that if there was a significant signal from MG 1019+0535, then the variance in pixels 1 and 2 would probably be larger than that in pixels 3 and 4. Also pixel 1 is expected to have an excess in measurement 2, and pixel 2 is expected to have an excess of measurement 1. Of these three conditions, only the very last is satisfied, but only weakly so, because pixel 4 has a higher reduced flux density in measurement 1 than has pixel 2. Thus it appears that the source is not detected in the $160 \mu\text{m}$ -band.

It is possible to derive an upper limit to the flux density by an analysis of these data, assuming the median flux densities are reasonably close to reality. The above data has a standard deviation of $\sigma = 0.016 \text{ MJy sr}^{-1}$. However, it is probable that the true background-subtracted pixel flux densities do not lie equidistant between the two measured background-subtracted and calibrated measurements in each pixel, as we have constructed it to be. That is, if our null hypothesis is correct, and there is no significant signal from MG 1019+0535, then the background-subtracted and calibrated measurements in each pixel are samples from a distribution of unknown mean, but which have been adjusted to give an artificial mean equidistant from the two measurements. A simulation showed that the intrinsic standard deviation is $\sigma = 0.022$. Thus the $1\text{-}\sigma$ upper limit on the existence of a signal from the source in a given pixel is $0.022 \text{ MJy sr}^{-1}$, or 4.2 mJy per pixel. This would be the $1 - \sigma$ upper limit of the source if its whole flux landed in one pixel. Because of the large airy disk at $160 \mu\text{m}$, if the source is in the center of a C200 pixel, then approximately 64% of the total flux at $160 \mu\text{m}$ lands in that pixel (Laureijs, 1999). This correction raises the 1-sigma constraint is $\sim 6.6 \text{ mJy}$. The 95% confidence upper limit on the flux density from MG 1019+0535 at $160 \mu\text{m}$ is thus $F_{160} \approx 13.2 \text{ mJy}$.

3.3. Submillimeter data for MG 1019+0535

Recent observations of AGN using IRAM at $1250 \mu\text{m}$ and JCMT (the James Clerk Maxwell Telescope, Mauna Kea, Hawaii) at $790 \mu\text{m}$ (Cimatti et al., 1998) provided the first positive measurements of dust associated with the radio galaxy MG 1019+0535. They find the flux at $790 \mu\text{m}$ is $14.70 \pm 4.60 \text{ mJy}$, and at $1250 \mu\text{m}$ it is $2.13 \pm 0.47 \text{ mJy}$. Published observations of synchrotron emission at longer wavelengths were cited that indicated that the possibility of contamination of their sub-millimeter observations was small and negligible in the observed 1250 and $790 \mu\text{m}$ wave-bands, respectively. The flux densities in these wave-bands confirmed that they were sampling the Rayleigh-Jeans part of the thermal dust-spectrum. Though these data do not enable a resolution of the temperature, Cimatti et al. (1998) thought it likely to be within the range $35 \leq T_d \leq 80 \text{ K}$, for the optically thin, and optically thick cases, respectively.

Using the sub-mm data of Cimatti et al. (1998), together with our estimated $2\text{-}\sigma$ upper-limit flux density of 13.2 mJy at an observed $160 \mu\text{m}$, we search for a least-squares fit to a Planck spectrum modified

by the assumed dust emissivity index $\epsilon = 2$. The resulting least-squares fit is consistent with a large FIR luminosity $\mathcal{L}_{FIR} \simeq 3.10 \times 10^{46}$ ergs s $^{-1}$, and an upper limit dust temperature of $T \sim 32.2$ K, which is below the range of the warm component of dust emission from star-forming galaxies (Calzetti et al., 2000). The 1- σ upper limit (i.e., 6.6 mJy) is fit by $T_d \leq 29.4$ K with a FIR luminosity $\mathcal{L}_{FIR} = 2.25 \times 10^{46}$ ergs s $^{-1}$.

Due to the extraordinary measures required to reduce the ISO data, it was thought prudent to check the reliability of our findings. In addition to serving this purpose, the following analysis of data for F 10214+4724, viewed as an AGN + starburst, may provide a glimpse of how MG 1019+0535 may have appeared at an earlier time.

3.4. ISO and IRAS data for F 10214+4724

The ultraluminous IRAS galaxy F 10214+4724 is a weak radio source with a Seyfert 2 nucleus and a circumnuclear starburst (Rowan-Robinson et al., 1993; ?; Lacy et al., 1998; Serjeant et al., 1998). It has been shown to be lensed (Graham & Liu, 1995; Broadhurst & Lehar, 1995; Downes et al., 1995), but remains one of the most intrinsically luminous galaxies known. Dey et al. (1995) noted that the Ly α line was extinguished by a factor greater than 40 relative to the He II λ 1640 line, though Serjeant et al. (1998) finds a double-peaked Ly α line with a total flux nearly equal to that of He II λ 1640, leading to an extinction ratio of only ~ 10 . Due to its non-spherically symmetric Seyfert 2 nature, we do not expect the Ly α to He II λ 1640 ratios to be as significant as with the radio galaxy MG 1019+0535 with respect to issues of dust distribution.

The ISO data for F 10214+4724 was taken in observing mode PHT32 by U. Klass (observation #14500967 and #14500968). This data has similar calibration problems to that of the PHT22 data, however, the over-sampling of this observing mode has resulted in a partial smoothing of the effects. Nevertheless there are still large systematic effects apparent on the maps, which take the form of patchy, systematically high or low values near the beginning or end of the raster mapping process. These spatially distinct fluctuations must have been caused by temporal fluctuations of sensitivity in this 3×1 raster map. The data is over-sampled in the “x” direction by the chopping, however it has only two pixels in the “y” direction. Figure 2 shows schematically the reduced 180, and 200 μ m data (left, and right sides of the figure, respectively) along these two lines of pixels. The galaxy is located on the line separating these two lines of pixels, and should have an equal contribution to each. The difference in the contributions of the upper and lower pair of pixels apparent in the upper pair of illustrations is attributable to calibration systematics between the pixel pairs. By carefully locating the source on the maps, we were able to mask out the area dominated by our source. We then fit a fourth-order polynomial to the remaining data, which was then subtracted from the data. The integrated flux density for the 180 and 200 μ m data was found to be 198, and 82 mJy, respectively. The large diameter of the airy disk for 180 and 200 μ m (151 and 168”, respectively) may have resulted in a significant fraction of the signal falling within the data used for fitting the polynomial model. For the 180, and 200 μ m measurements, the airy disk extends to 5.9 and 7.0 sub-pixel units (see Fig. 2) to either side of the peak of the emission, respectively, whereas only a total of 8 pixels were blocked out in the fitting of the continuum. Because this process could only over-estimate the background, our reduced fluxes should be considered lower bounds on the flux densities.

The IRAS data for F 10214+4724 shows a flux density of 204 ± 46 , and 580 ± 150 mJy in the 60 and 100 μ m-bands, respectively, as retrieved on NED (Jan., 2000). By transforming to F_λ , we find almost identical fluxes ($F_\lambda \approx 1.70 \pm 0.40$, and $1.76 \pm 0.44 \times 10^{-17}$ ergs s $^{-1}$ \AA^{-1} , respectively). We fit these values

to a Planck spectrum with an emissivity index $\epsilon = 2$ by placing them on opposing sides of the maximum, and using the spectral responsivities of the 60 and 100 μm filters (available from the Goddard Space Flight Center web-site), we derive a normalization and temperature which are consistent with the observed fluxes. We find $T_d \simeq 89 \pm 12$ K, and integrated from 1 to 500 μm , the attributed FIR luminosity is $\mathcal{L}_{FIR} \simeq 7.4 \pm 0.8 \times 10^{47}$ ergs s $^{-1}$. However, observations at the JCMT (Rowan-Robinson et al., 1993) at 450 and 800 μm , show this model is an order of magnitude low in F_ν . This excess over the model suggests a massive, but cooler cloud ($T_d \approx 30$ K).

Analysis indicates that the FIR luminosity is magnified by ~ 13 times (Downes et al., 1995). Neglecting the luminosity contributed by the cooler cloud, this leads to a more modest FIR luminosity $\mathcal{L}_{FIR} \approx 5.7 \pm 0.6 \times 10^{46}$ ergs s $^{-1}$. When the fit is extended to the 180 and 200 μm bands we find the ISO data is $\sim 55\%$, and $\sim 27\%$ lower than that predicted by the fit, respectively, for the central value of the temperature, but they are only modestly low when the higher side of the $1 - \sigma$ temperature range is used. It is probable that the ISO data appears low because the background continuum level was over-estimated, as noted above. Thus, with these caveats, the ISO fluxes appear consistent with IRAS fluxes, at least to within a factor of two. We conclude that the upper limits on F_{160} for MG 1019+0535 (§3.2) can be accepted with confidence.

3.5. ISO and Sub-millimeter Data for TXS 0211–122

Because the modestly lower redshift of TXS 0211–122 ($z_{em} = 2.300$) would place the 160 μm band closer to the maximum on the Wien side if its dust cloud had a temperature close to that of MG 1019+0535, it was hoped that a detection was possible. The TX 0211–122 data (G. Miley, TDT 59601713) at 160 μm was observed in the same P32 raster mapping mode as F 10214+4724. We followed the same procedures for reducing the data (see §3.4). However, systematic effects overwhelmed the data, and no signal was detected. It was not possible to carry out the specialized reduction procedures used for MG 1019+0535. Observations by Cimatti et al. (1998) with SEST (Swedish-ESO Submillimetre Telescope) were unable to detect the galaxy at 1270 μm ($S_\nu = -0.53 \pm 3.99$ mJy), but they provided a $1-\sigma$ upper limit comparable to the 1-sigma upper limit on the detection of MG 1019+0535 at 1250 μm . Thus, constraints on the dust temperature and luminosity are not as severe as those on MG 1019+0535 by this analysis. We note, however, that of the three galaxies discussed here, TXS 0211–122 has the least amount Ly α quenching in relation to He II λ 1640 or C IV λ 1549 (Dey et al., 1995) (a factor of ~ 6.5 rather than ~ 10).

4. Reconciling the FIR with Optical Data

We now discuss the reasonableness of the upper limit temperatures and luminosities of MG 1019+0535 and F 10214+4724 in the light of plausible values for parameters and features characterizing their optical spectra.

4.1. F 10214+4724

In the case of F 10214+4724, Rowan-Robinson et al. (1991) note that the optical plus ultraviolet fluxes account for less than 1% of the total bolometric output of the galaxy ($\sim 0.5\%$ according to Serjeant et al.

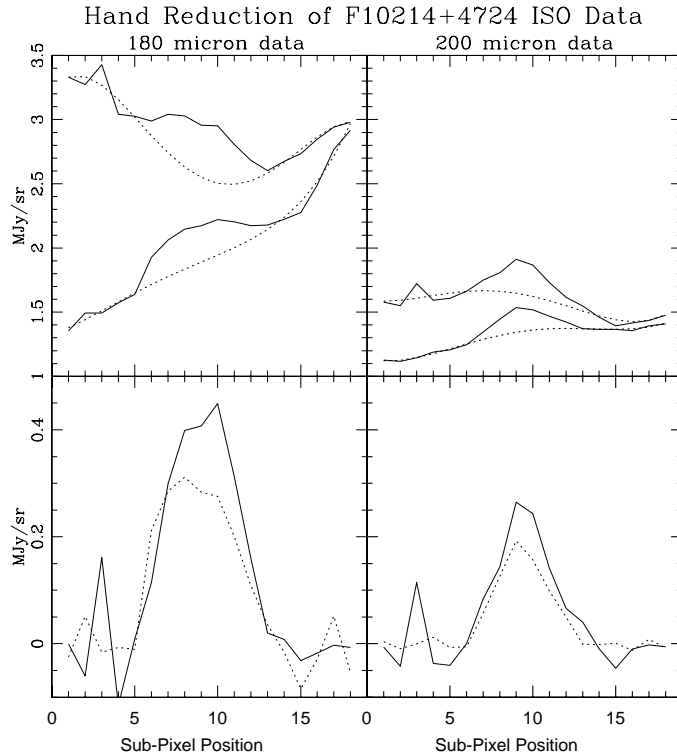


Fig. 2.— The flux-calibrated emission in the two lines of pixels from the 3×1 raster map of F 10214+4724 ISO data in 180 and 200 μm (upper left and right, respectively). In the upper plots, the solid line represents the data, and the dotted lines represent the 4-th order polynomial fit made by considering the points between pixels 1 through 5 and 14 and 18. In both cases the summed flux from the top row of pixels (numbers 1 and 4 in Fig. 1) have the higher counts. The bottom two panels show the fit subtracted from the data, where the solid lines represent the top row of pixels, and the dotted lines represent the contributions of pixels 2 and 3. This systematic difference again hints at unremoved systematic errors. One can sense that the extracted fluxes are lower limits, as the wings of the PSF were included in the data for the continuum fit (see text).

(1998)). This implies $\mathcal{L}_{FIR} \approx \mathcal{L}_{bol} \approx 5.7 \times 10^{46} \text{ ergs s}^{-1} \approx \mathcal{L}_{int}$, the intrinsic luminosity. This luminosity is a factor of ~ 2 greater than that found by Serjeant et al. (1998) based on the $H\alpha$ flux in conjunction with the magnification estimates of Downes et al. (1995). The observed spectral slope in UV-bright, local star forming galaxies is found to be dependent on their color excess (Kinney et al., 1993). If we use this relation as a guide, then the extinction data from F 10214+4724 implies a spectral slope, defined by $F_\lambda \propto \lambda^\beta$, of $\beta \gtrsim 0.5$, and $E_{B-V} \gtrsim 0.55$. The slope β is large because it has been reddened by extinction. In this case, the intrinsic optical spectrum is energetically depleted by $\gtrsim 99\%$. In light of the high dust temperature found for this object, and its starburst nature, it is reasonable to suppose that the dust is physically close to the sources of emission. As noted by Chen & Neufeld (1994), the warm dust component surrounds OB associations and HII regions, and attenuates the continuum, and may preferentially attenuate the LyA line if H I is present. A cool component is expected, but is undetected in the $\lambda \leq 1250 \mu\text{m}$ data. It may be seen in the excess of the 450 and 800 μm data (Rowan-Robinson et al., 1993) relative to the single-temperature model (§3.4).

4.2. MG 1019+0535

What signs of optical extinction are there for MG 1019+0535? For a post-starburst galaxy, the OB associations and HII regions are absent. The dust is now cool. Dey et al. (1995) note that the decrease in the ratio of N V λ 1240 to He II λ 1640 relative to the 3CR composite of McCarthy (1993) can be explained by a large color excess $E_{B-V} = 0.3 - 0.4$. But is this reasonable? In order to calculate the extinction in the optical, we require an estimate of the observed continuum luminosity, a spectral slope, and a color excess. The former can be extracted using the flux in the redshifted line $F_\alpha = 8.4 \pm 0.6 \times 10^{-17}$ ergs cm $^{-2}$ s $^{-1}$ and its observed equivalent width $W_\lambda^{obs} = 268$ Å (Dey et al., 1995), leading to a continuum flux density $F_C = 3.13 \pm 0.22 \times 10^{-19}$ ergs cm $^{-2}$ s $^{-1}$ Å $^{-1}$. Transformed to a continuum luminosity at $z = 2.765$, we find $\mathcal{L}_C(\alpha) = 6.80 \pm 0.49 \times 10^{40}$ ergs s $^{-1}$ Å $^{-1}$. The “observed” continuum depends on the spectral slope β and our continuum luminosity at rest λ 1216 Å. By increasing the slope we find that the continuum luminosity increases. This rather counter-intuitive result follows from the fact that we are extrapolating the continuum from the point at rest λ 1216 Å.

We calculate the extinction in optical wavelengths in order to estimate the FIR luminosity that might result; the difference between the unextinguished, and the observed continuum luminosity should approximate the FIR luminosity. The continuum optical energy lost in extinction can be calculated by the integral, adapted from Calzetti et al. (1994),

$$\Delta\mathcal{L}_{ext} = \mathcal{L}_C(\alpha) \int_{0.1 \mu\text{m}}^{0.6} \left\{ \left(\frac{\lambda}{0.1216 \mu\text{m}} \right)^\beta 10^{0.4 E_{B-V} k(\lambda)} - 1 \right\} d\lambda \text{ ergs s}^{-1}, \quad (1)$$

where $k(\lambda)$ is a polynomial valid for Galactic extinction, λ is expressed in μm , and \mathcal{L}_C is the continuum luminosity at the Ly α line, given above. If we treat MG 1019+0535 as a starburst galaxy and use the values $\beta \approx -0.5$ and $E_{B-V} \approx 0.5$ consistent with the Kinney et al. (1993) relation for star-forming galaxies, we can reproduce the N V λ 1240 to He II λ 1640 ratio observed by Dey et al. (1995). However, only $\sim 2.5\%$ of the continuum between $0.11 \mu\text{m} \leq \lambda \leq 0.6 \mu\text{m}$ would be unextinguished. Even so this FIR luminosity would imply a $160 \mu\text{m}$ flux within even the $1-\sigma$ detection limits in the ISO $160 \mu\text{m}$ -band. However, in that case, the intrinsic Ly α line would be huge: To calculate the intrinsic Ly α line luminosity, the observed $\mathcal{L}_\alpha^{obs} = 4.84 \times 10^{42}$ ergs s $^{-1}$ must not only be corrected by a factor of ~ 10 for the low line-strength of Ly α relative to He II λ 1640, but also for the extinction at the He II λ 1640 line, calculated using the derivative of Eq. 1. In this case there is a combined factor of ~ 130 , leading to a predicted intrinsic line luminosity of $\mathcal{L}_\alpha = 6.3 \times 10^{44}$ ergs s $^{-1}$. This is larger than the highest Ly α line luminosity in a sample of 165 high-redshift radio galaxies (De Breuck et al., 2000), and roughly an order of magnitude larger than the mean at $z \simeq 2.7$. If we constrain the intrinsic Ly α line of MG 1019+0535 to be less than a more moderate luminosity $\mathcal{L}_\alpha = 1.6 \times 10^{44}$ ergs s $^{-1}$ (a value greater than $\sim 88\%$ of Ly α line luminosities in Fig. 8 of De Breuck et al. (2000)), then in effect, the unextinguished, or observed fraction of photons at rest wavelength ~ 1640 Å must be $\gtrsim 1/3$. For $\beta = 0$, this requires $E_{B-V} \approx 0.12$. For these values of β and E_{B-V} we find the energy absorbed by dust to be a modest $\mathcal{L}_{ext} \simeq 4.2 \times 10^{44}$ ergs s $^{-1}$, and an intrinsic optical luminosity between $0.11 \mu\text{m} \leq \lambda \leq 0.6 \mu\text{m}$ of $\mathcal{L}_{opt}^{int} \simeq 7.5 \times 10^{44}$ ergs s $^{-1}$. These parameters would not give the observed N V λ 1240 to He II λ 1640 ratio of 0.27 (it produces a ratio 0.45), but we believe that the uncertainty in this line ratio, both in MG 1019+0535 and the composite, is large due to the weakness of the N V λ 1240 line. An intrinsic slope of $\beta \simeq 0$ is consistent with the spectral energy distribution of a 500 Myr old starburst with solar metallicity (Leitherer et al., 1999).

How confident are we of these values? We have until now neglected the effect of the uncertainties in the sub-millimeter data (see §3.3). We find that the maximal effect of independently varying

the values found in the sub-millimeter bands over their $\pm 1\text{-}\sigma$ range of uncertainties (Cimatti et al., 1998), which are on the order $\sim 20 - 30\%$, is slight. For example, if $F_{160} = 2.0$ mJy, we find that $T_d = 25.6 \pm 0.6$ K, and $\mathcal{L}_{FIR} = 1.43 \pm 0.20 \times 10^{46}$ ergs s^{-1} . For $F_{160} = 0.02$ mJy, $T_d = 19.2 \pm 1.2$ K, and $\mathcal{L}_{FIR} = 6.33 \pm 0.38 \times 10^{45}$ ergs s^{-1} , (still about an order of magnitude greater than that which would result from $E_{B-V} = 0.12$). Since the uncertainties apparently remain modest and relatively uniform over the parameter range investigated here, the uncertainties in the sub-millimeter observations can have no significant effect on our argument that the dust cloud in MG 1019+0535 is cool.

In seeking a concordance, we have found that we must accept a larger intrinsic Ly α luminosity with the larger FIR luminosity when we increase E_{B-V} . To keep the intrinsic Ly α luminosity of MG 1019+0535 from being extraordinarily large, we find we must propose a modest color excess $E_{B-V} \approx 0.12$. But then we must live without the explanation for the observed N V $\lambda 1240$ to He II $\lambda 1640$ ratio.

5. Discussion

Based on our FIR single-temperature fit, the lens-corrected bolometric luminosity of F 10214+4724 is $\mathcal{L}_{tot} \gtrsim 5.7 \times 10^{46}$ ergs s^{-1} . The higher temperature of the dust, and the highly energetic nature of the galaxy can be easily be reconciled with a strong concurrent starburst, while the temperature of MG 1019+0535 can be reconciled with a *post*-starburst galaxy. The lack of detection of TXS 0211–122 in the FIR is not unexpected since the $1\text{-}\sigma$ upper limit to the flux at $1270 \mu\text{m}$ is larger than the detection at $1250 \mu\text{m}$ for MG 1019+0535, which, after all, has a Ly α line more strongly diminished in relation to its He II $\lambda 1640$ line (Dey et al., 1995).

These galaxies appear to be detectable in the FIR in proportion to the degree in which their Ly α lines are suppressed (see §1), though the recent observations by Serjeant et al. (1998) may indicate that the Ly α line of F10214+4724 is ~ 4 times stronger than that reported by Dey et al. (1995). But on the other hand, the nuclear spectrum of this Seyfert 2 galaxy may have a lower average extinction than the continuum (Serjeant et al., 1998). It also appears that dust temperature may be positively correlated with the relative amount of extinction in our sample. Below we discuss these issues in terms of the general properties of passively evolving starburst galaxies, and then discuss the prospects for getting a true measurement of the dust temperature and FIR luminosity for our two radio bright galaxies.

5.1. General properties

The increased frequency with which radio galaxies are found to be observable in the $850 \mu\text{m}$ band as one probes higher redshifts (Archibald et al., 2000) prompts us to speculate that the epoch of the formation of the majority of radio galaxies is being probed (i.e., $z = 3 - 5$). The presence of dust, albeit *cool* dust, in MG 1019+0535 suggests that this radio galaxy is relatively young, yet decidedly *post*-starburst. The starburst IRAS galaxy F 10214+4724 is found to have quite warm dust ($T_d \approx 89$ K) and its optical luminosity is almost totally extinguished. An interesting “in between” case may be the galaxy NGC 5860 (MRK 0480), which was found to have a FIR spectrum consistent with a single temperature $T_d \simeq 32$ K (Calzetti et al., 2000). This galaxy has been identified as a “fading” starburst (Mazzarella & Boroson, 1993), and hence may plausibly be construed as supporting the position that the lack of a warm component (i.e., $40 \lesssim T_d \lesssim 55$ K) signifies a significant stretch of time between active star formation in the galaxy, and the epoch of the observation.

As noted by Calzetti et al. (2000), the dust mass involved in the cool component of star-forming galaxies can be up to 150 times that associated with the warm component, even though their warm component is usually more luminous. Thus the absence of a detected warm component in MG 1019+0535 (or in NGC 5860) suggests that the dust mass present in any undetected warm component is truly insignificant compared to the mass of the cool dust.

5.2. Modeling dust temperatures

For a galaxy formed by an instantaneous burst, the mass ejection rate is thought to reach a maximum dominated by supernovae within the first ~ 40 Myr, followed by a steep decline of nearly two orders of magnitude (Leitherer et al., 1999). After this period, the mass ejection rate is well approximated as halving as age doubles (a power law slope of ~ -1). However, the luminosity is seen to decline at a quite similar rate. Therefore attributing the lowered FIR luminosity for aged radio galaxies to a dispersal of dust, rather than a decline in galaxy luminosity, is not straightforward. We can, however, compound a simple model of the dust temperature as a function of distance and time since the burst (starting, that is, at an age, $t_0 \simeq 40$ Myr). For dust clouds well-approximated by a single temperature (as with F 10214+4724), this seems defensible. Further, we note that the strong correlation of UV line luminosities and equivalent widths in high-redshift radio galaxies implies that the source powering the narrow line region is dominated by a common energy source (De Breuck et al., 2000). We adapt the analysis of Finkbeiner et al. (1999) regarding the equilibrium dust temperature to dust at a variable distance r from a source with a given source luminosity characterized by a temperature T_S . The dust temperature should be well-approximated by the relation,

$$T_d \propto \frac{T_S^{4/(4+\epsilon)}}{r^{2/(4+\epsilon)}}, \quad (2)$$

where r is the distance from the energy source, and the emissivity index is assumed to be a constant $\epsilon = 2$. This model shows that dust with $T_d \sim 20$ K must lie at a distance ~ 80 times greater than dust with $T_d \sim 90$ K. For instance, if dust at 90 K is 5 kpc from the source, the dust at 20 K would be at 400 kpc. However, if we accept that the luminosity of the galaxy declines approximately with the inverse first power of time t since the end of the burst, as we noted above, but keep T_S constant, then

$$T_d \propto (r^2 t)^{-1/(4+\epsilon)}. \quad (3)$$

This equation allows us to check the hypothesis that dust is not expelled, but that temperature differences are due to the passive evolution of the energy source. If the distance of the dust is unchanged, we find that it would take $t > 300$ Gyr for a dust cloud of temperature 90 K to become a 20 K cloud under passive evolution of the galaxy for a constant T_S . Including a plausible reduction in T_S to half its initial value results in $t > 18$ Gyr. This suggests that the principal cause of the cooler dust in MG 1019+0535 is the outward movement of the dust cloud, rather than passive evolution of the galaxy. This result, it must be acknowledged, comes about by equating the observed nature of F 10214+4724 as comparable to what MG 1019+0535 must have been like near the end of the starburst which formed it. Though these galaxies are different in many respects, we believe they are comparable from the standpoint of the temperature of the dust in a passively evolving starburst galaxy. We note that the passive evolution of a galaxy with the apparent (lensing corrected) bolometric luminosity of F 10214+4724 over 700 Myr could very plausibly result in a luminosity similar to that attributed to MG 1019+0535 (Leitherer et al., 1999).

If we now allow that the cloud is being blown away at a constant velocity $v \sim 500$ km s $^{-1}$, as suggested from the redshift of the Ly α line relative to He II λ 1640, C IV λ 1549, and C III λ 1909 (Dey et al., 1995;

Legrand et al., 1997; Kunth et al., 1998), then substitution of $r = r_0 + vt$ allows us to solve for the post-starburst age of the galaxy and the galactocentric distance of the dust cloud as a function of dust temperature. Given a dust cloud of ~ 90 K, assumed to be observed at a galactocentric radius of $r_0 = 5$ kpc (roughly half of the isophotal radius of the R-band image of MG 1019+0535 in Dey et al. (1995)), then a $T_d = 20$ K cloud could be explained if the galaxy had evolved passively for ~ 700 Myr. During this time, the cloud would move to a distance of $r \simeq 360$ kpc. Such a galaxy, if seen at the redshift of MG 1019+0535 ($z = 2.765$), would have been formed at $z \simeq 4.3$, or 3.2, for our assumed cosmology (§1), or a flat universe with $h = 0.7$ and $\Lambda = 0.7$, respectively. Therefore, the naive conclusion that cool dust clouds (in evolved galaxies lacking a warm component) are more distant than the warm components of starburst, or fading starburst galaxies, appears consistent with our findings, and supports the view that dust in post-starburst galaxies is blown to large galactocentric radii by superwinds, photon pressure, or corpuscular drag.

5.3. Future prospects

In order to settle the still significant uncertainties regarding the radio galaxy MG 1019+0535 and TXS 01211-122, it would be advisable to observe these objects near the projected maxima of their FIR spectra, in the observed $\lambda \sim 250 - 500 \mu\text{m}$. While SIRTf may be useful to chart the movement of dust at redshifts out to $z \approx 1$, its wavelength coverage and angular resolution will not be sufficient to resolve the mysteries associated with MG 1019+0535 and TXS 0211-122. SOFIA will have good angular resolution, but broad-band spectral coverage stops short of the projected maximum for MG 1019+0535. However, it may be detectable if our conclusion that $T_d \lesssim 20$ K is incorrect. For definitive data we will probably have to wait until the launch of ESA’s FIRST (Far InfraRed Space Telescope), which will incorporate the bolometer instrument SPIRE, which combines a camera and spectrometer. It will probe point-sources to a sensitivity $F_\nu \lesssim 1$ mJy in three broad bands centered on 250, 350, and 500 μm simultaneously by the use of dichroic filters, and have the spatial resolution needed to remove much of the galactic cirrus. The launch date is currently 2007.

6. Conclusions

We suggest the following conclusions:

- MG 1019+0535 is accompanied by a decidedly *cool* dust cloud, of a temperature cooler than $T_d \lesssim 20$ K, and a low color excess in the range, $E_{B-V} \approx 0.12$, if its intrinsic Ly α line is not unusually luminous, but most probably no greater than twice that. It is likely that its bolometric luminosity is $\mathcal{L}_{tot} \lesssim \text{few} \times 10^{45}$ ergs s $^{-1}$, consistent with ~ 700 Gyr of passive evolution from a galaxy with on order the apparent luminosity of F 10214+4724.
- The IRAS galaxy F 10214+4724 was found to have a dust temperature $T_d \simeq 89 \pm 12$ K, and a high FIR luminosity, $\mathcal{L}_{FIR} \approx 5.7 \pm 0.6 \times 10^{46}$ ergs s $^{-1}$, close to its bolometric luminosity.
- The non-detection of TXS 0211-1122 in either the 160 μm -band, or in the sub-mm at 1270 μm suggests that it has a comparable or lower FIR luminosity and dust temperature than MG 1019+0535, in line with its 50% larger Ly α to He II λ 1640 line flux ratio.
- The trend of high dust temperatures in starbursts, and low temperatures in post-starburst galaxies is suggestive of dust having a larger mean distance for evolved galaxies. We speculate that the principal

reason for this is a combination of two factors – first, that dust is transported to larger galactocentric radii by various mechanisms including photon pressure, corpuscular drag, and superwinds, and second, the mass ejection rate \dot{M} declines rapidly for a post-starburst galaxy of age $t \gtrsim 40$ Myr. The lack of a “warm” dust component in a post-starburst galaxy is then due to the steep decline in mass ejection rate at ~ 40 Myr post-starburst.

We wish to thank Nanyao Lu and the staff at IPAC for hospitality and assistance during our stay in Pasadena. We benefitted from helpful suggestions from Arjun Dey, Douglas Finkbeiner, Daniel Stern, and Wil Van Breugel. We received very helpful suggestions from the anonymous referee. We are grateful to NASA/ISO/JPL for financial support (contract #961501).

REFERENCES

- Archibald, E. N., Dunlop, J. S., Hughes, D. H., Rawlings, S., Eales, S. A., & Ivison, R. J. 2000, MNRAS, in press; astro-ph/0002083
- Broadhurst, T. & Lehar, J. 1995, ApJ, 450, L41
- Burns, J. A., Lamy, P. L., & Soter, S. 1979, Icarus, 40, 1
- Calzetti, D. 1999, in *Building the Galaxies: from the Primordial Universe to the Present*, ed. F. Hammer, T. X. Thuan, V. Cayatte, B. Guiderdoni, & J. T. Thanh Van, in press
- Calzetti, D., Armus, L., Bohlin, R. C., Kinney, A. L., Koornneef, J., & Storchi-Bergmann, T. T. 2000, ApJ, 533, 682
- Calzetti, D., Kinney, A. L., & Storchi-Bergmann, T. 1994, ApJ, 429, 582
- Chen, W. L. & Neufeld, D. A. 1994, ApJ, 432, 567
- Cimatti, A., Freudling, W., Rottgering, H. J. A., Ivison, R. J., & Mazzei, P. 1998, A&A, 329, 399
- De Breuck, C., Rottgering, H., Miley, G., van Breugel, W., & Best, P. 2000, A&A, in press, astro-ph/0008264
- Dey, A., Spinrad, H., & Dickinson, M. 1995, ApJ, 440, 515
- Downes, D., Solomon, P. M., & Radford, S. J. E. 1995, ApJ, 453, L65
- Finkbeiner, D. P., Davis, M., & Schlegel, D. J. 1999, ApJ, 524, 867
- Frye, B. & Broadhurst, T. 1998, ApJ, 499, L115
- Graham, J. R. & Liu, M. C. 1995, ApJ, 449, L29
- Kinney, A. L., Bohlin, R. C., Calzetti, D., Panagia, N., & Wyse, R. F. G. 1993, ApJS, 86, 5
- Kunth, D., Mas-Hesse, J. M., Terlevich, E., Terlevich, R., Lequeux, J., & Fall, S. M. 1998, A&A, 334, 11
- Lacy, M., Rawlings, S., & Serjeant, S. 1998, MNRAS, 299, 1220
- Laureijs, R. J. 1999, http://www.iso.vilspa.esa.es/users/expllib/PHT_top.html, Additional PHT Documents, the fifth article

- Legrand, F., Kunth, D. F., Mas-Hesse, J. M., & Lequeus, J. 1997, *A&A*, 326, 929
- Leitherer, C., Schaerer, D., Goldader, J. D., Delgado, R. M. G. ., Robert, C., Kune, D. F., de Mello, D. F., Devost, D., & Heckman, T. M. 1999, *ApJS*, 123, 3
- Lonsdale Persson, C. J. & Helou, G. 1987, *ApJ*, 314, 513
- Matthews, T. A., Morgan, W. W., & Schmidt, M. 1964, *ApJ*, 140, 35
- Mazzarella, J. M. & Boroson, T. A. 1993, *ApJS*, 85, 27
- McCarthy, P. J. 1993, *ARA&A*, 31, 639
- McLure, R. J., Kukula, M. J., Dunlop, J. S., Baum, S. A., O’Dea, C. P., & Hughes, D. H. 1999, *MNRAS*, 308, 377
- Neufeld, D. A. 1991, *ApJ*, 370, L85
- Rowan-Robinson, M., Broadhurst, T. J., Lawrence, A., McMahon, R. G., Lonsdale, C. J., et al. 1991, *Nature*, 351, 719
- Rowan-Robinson, M., Efstathiou, A., Lawrence, A., Oliver, S., Taylor, A., Broadhurst, T. J., McMahon, R. G., Benn, C. R., Condon, J. J., Lonsdale, C. J., Hacking, P., Conrow, T., Saunders, W. S., Clements, D. L., Ellis, R. S., & Robson, I. 1993, *MNRAS*, 261, 513
- Serjeant, S., Rawlings, S., Lacy, M., McMahon, R. G., Lawrence, A., Rowan-Robinson, M., & Mountain, M. 1998, *MNRAS*, 298, 321
- Warren, S. J., Iovino, A., Hewett, P. C., & Shaver, P. A. 1998, *MNRAS*, 299, 1215